

# Q2237+0305 source structure and dimensions from light curves simulation

V. G. Vakulik<sup>1</sup>, R.E.Schild<sup>2</sup>, G.V.Smirnov<sup>1</sup>, V.N.Dudinov<sup>1</sup>, V.S.Tsvetkova<sup>3</sup>

<sup>1</sup>*Institute of Astronomy of Kharkov National University, Sumskaya 35, 61022 Kharkov, Ukraine*

<sup>2</sup>*Center for Astrophysics, 60 Garden Street, Cambridge, MA 02138, U.S.A.*

<sup>3</sup>*Institute of Radio Astronomy of Nat.Ac.Sci. of Ukraine, Krasnoznamenaya 4, 61002 Kharkov, Ukraine*

*Email: vakulik@astron.kharkov.ua, rschild@cfa.harvard.edu, gleb.smirnov@gmail.com, dudinov@astron.kharkov.ua, tsvetkova@astron.kharkov.ua*

Accepted ... Received ...; in original form 2006 August 11

## ABSTRACT

Assuming a two-component quasar structure model consisting of a central compact source and an extended outer feature, we produce microlensing simulations for a population of star-like objects in the lens galaxy. Such a model is a simplified version of that adopted to explain the brightness variations observed in Q0957 (Schild & Vakulik 2003). The microlensing light curves generated for a range of source parameters were compared to the light curves obtained in the framework of the OGLE program. With a large number of trials we built, in the domain of the source structure parameters, probability distributions to find "good" realizations of light curves. The values of the source parameters which provide the maximum of the joint probability distribution calculated for all the image components, have been accepted as estimates for the source structure parameters. The results favour the two-component model of the quasar brightness structure over a single compact central source model, and in general the simulations confirm the Schild-Vakulik model that previously described successfully the microlensing and other properties of Q0957. Adopting 3300 km/s for the transverse velocity of the source, the effective size of the central source was determined to be about  $2 \cdot 10^{15}$  cm, and  $\varepsilon \approx 2$  was obtained for the ratio of the integral luminosity of the outer feature to that of the central source.

**Key words:** cosmology: gravitational lensing – galaxies: quasars: individual: QSO 2237+0305.

## 1 INTRODUCTION

Because quasar microlensing has the potential to reveal details about the structure of quasars, large observational data bases at X-ray, optical, and even radio wavelengths have been assembled for the Q2237+0305 system to compare to theoretical models. The approaches to infer microlensing parameters from the light curves of the Q2237 image components may be divided into two classes. One of them is based upon the analysis of individual microlensing events interpreted as crossing of a caustic fold or cusp by the source (e.g., Webster et al. 1991, Shalyapin 2002, Yonehara 2001, Gil-Merino et al. 2006). The second approach referred hereafter as the statistical one, utilizes all the available observational data to infer the intrinsic statistical parameters. This approach is represented, e.g., by the structure function analysis by Lewis and Irwin (1996), or the analysis of distribution of the Q2237 light curve derivatives by Wyithe, Webster & Turner (1999, 2000). Recently, Kochanek (2004) applied a method of statistical trials to analyse the well-sampled light curves of Q2237 obtained in the framework of the OGLE monitoring campaign.

Both approaches have their intrinsic weak points and advantages. In particular, in analysing an individual microlensing event, it is necessary to presume that the source actually crosses a single caustic, and that the source size is significantly smaller than the Einstein radius of typical microlenses. Moreover, there must be some complexity caused by the unknown vector difference between the microlens trajectory and the macrolens shear.

In applying the statistical approach, the microlensing parameters are obtained through the analysis of the lensed light curves as a whole, and much less specific assumptions on the microlensing event peculiarities are needed. This approach may encounter the problem of insufficiency of statistics, however, and Q2237 is just the case: according to Wambsganss, Paczyński & Schneider (1990) and Webster et al. (1991), light curves of duration more than 100 years are needed to obtain reliable statistical estimates of microlensing parameters.

The mechanism of accretion onto the massive black hole is presently believed to provide the most efficient power supply in AGNs (quasars), and effectively all researchers uses various accretion disk models when interpreting microlensing events in

gravitationally lensed quasars, e.g. Rauch & Blandford (1991), Jaroszyński, Wambsganss and Paczyński (1992), and more recent publications by Yonehara (2001), Shalyapin et al. (2002), Gil-Merino et al. (2006). However, with the accretion disc being generally accepted as a central engine in quasars, the difficulties in explaining the observed polarization and spectral properties of quasar radiation and their variety still remain, (Ferland & Rees 1988, Laor & Netzer 1989), as well as the amplitudes of the long-term microlensed light curves, which we will discuss in the present paper.

To explain these discrepancies, some additional structural elements are introduced. Outer structural elements inferred are an envelope of high-velocity clouds or wind re-emitting the hard chromospheric X-ray energy as a network of broad emission lines, and an equatorial torus containing the dark clouds that re-absorb the radiation emanating in some directions (Antonucci 1993). But the persistent broad blue-shifted emission lines previously explained by Antonucci (1993) as an envelope of high-velocity clouds have persisted for such a long time in any quasar that they must be explained as outflows. Despite many years of the idea of outflows, (Chelouche 2005 and references therein), the physics of the outflows is not clearly understood as yet. Elvis (2000) has suggested the outflow as being launched from the central region of quasars and thus, has successfully described how a simple outflow structure can explain the emission lines in virtually all quasars. The impulse timing analysis of the emission lines by Kaspi et al. (2000) for 17 quasars shows that the size scale for these structures must be comparable to the size scales implied by auto-correlation analysis for continuum radiation by Schild (2005, Fig.1), so it appears that the Elvis structures may be expected to originate a significant fraction of the quasar's UV-optical luminosity. Direct microlensing measurement of the thickness size scale of the emission line emitting region in SDSS1004+41 (Richards 2004) implies a size scale comparable to the continuum emitting region thickness scale (Schild, Leiter, Robertson 2006).

There is observational evidence for the existence of these extended structures in the Q2237+0305 quasar. Mid-infrared observations of Q2237 made by Agol et al. (2000) favor the existence of a shell of hot dust extending between 1 pc and 3 pc from the quasar nucleus and intercepting about half of the QSO luminosity. The flux ratios of the four Q2237 macroimages measured at 3.6  $\mu$ m and 20  $\mu$ m by Falco et al. (1996) were also interpreted as originating in a source much larger than that radiating in the optical wave lengths. Observations in the broad emission lines also suggest that they originate in a very large structure in Q2237, much larger than that emitting the optical continuum, (Lewis et al. 1998, Racine 1992, Saust 1994, Mediavilla et al. 1998), though the most recent observations by Wayth et al. (2005) indicate a much smaller BEL region, perhaps three times larger than the continuum region. We find that the Elvis (2000) outflow model easily accommodates these observations.

Microlensing light curves of these complicated source structures may noticeably differ from those for a simple source structure represented by an accretion disk alone. In particular, the accretion disk alone cannot reproduce in simulation the observed amplitudes of the Q2237 light curves. While providing good fits for the peaks, which are most sensitive to the effect of the central source, it fails to provide the actual amplitudes of the rest of the light curves, (Jaroszyński et al. 1992). In this respect, the results by Yonehara (2001), Shalyapin et al. (2002), and Gil-Merino et al. (2006) who analysed the regions of the light curves near the peaks of HME, provide successful estimates of the central source, but ignore the effect of a possible quasar outer feature.

It should be noted that as early as 1992, Jaroszyński, Wambsganss and Paczyński admitted existence of an outer feature of the quasar, that reprocesses emission from the disk and may contribute up to 100% light in *B* or *V*. They simulated microlensed light curves for the thin thermal accretion disk model. A bit later, Witt & Mao (1994) demonstrated in their simulations of microlensed light curves of Q2237, that a source model consisting of a small central source surrounded by a much larger halo structure, would better explain the observed amplitudes of the Q2237 light curves.

Also, the existence of one or several "hot spots" arising in the accretion disk was discussed by Gould and Miralda-Escudé (1997), and supported by Schechter et al. (2003) later, in their analysis of the HE1104-1805 light curves. Recently, it has been shown how the microlensing light curves may be affected by a presumed fractal structure in the X-ray emitting region (Lewis 2004), and in the broad line region (Lewis & Iбата 2006). In 2003, Schild & Vakulik have shown how the double-ring model of the Q0957 surface brightness distribution, resulting from the Elvis (2000) quasar spatial structure model, successfully explains the rapid low-amplitude brightness fluctuations in Q0957+561. Reference to microlensing models of Schild and Vakulik (2003) allowed inferences about structure sizes, and Schild (2005) even showed that the orientation of the quasar on the plane of the sky can be determined. Interestingly, Abajas et al. (2002, 2007) have recently simulated the emission line and continuum light curves produced by microlensing of a bi-conic outflow region for a variety of the bicone orientations with respect to the shear, direction of motion and sight line.

The standard accretion disc model also cannot explain the large color effects associated with microlensing discovered by Vakulik et al. (2004). Color variations in microlensing of an accretion disc with a radial temperature-color gradient have been predicted by Kayser, Refsdal & Stabell (1986) and simulated later by Wambsganss and Paczyński (1991). An excellent and careful simulation by Jaroszyński, Wambsganss, & Paczyński (1992) showed that microlensing color effects comparable to those observed are possible with their classical geometrically thin, optically thick accretion disc model, but they predicted a rather small source and too large brightness fluctuations in the simulated light curves.

In the sections to follow, we analyse the Q2237 microlensing light curves using a two-component model of the quasar's structure, and apply a statistical approach to determine parameters of this two-component source model. The approach we applied is in general similar to that of Kochanek (2004). In contrast to our ring model proposed earlier (Schild & Vakulik 2003), we used a simplified model, consisting of a compact central source and an extended outer structure with a much smaller surface brightness. Such a model, being much easier for calculations, possesses the principal property of the ring model to produce sharp peaks of the simulated light curves, while damping the amplitudes of the entire microlensing event light curve.

Thus, our basic approach is to accept the existence of inner and outer structural elements as detailed above, and to derive from parameter fitting only the size of the inner luminous feature, and the fraction of the total UV-optical energy from the extended outer feature as compared to the luminosity originating in the compact central feature. We will show that the structural elements of this two-component quasar model satisfactorily explain the observed microlensing brightness curves.

## 2 SIMULATION OF LIGHT CURVES

In the vicinity of a selected macroimage, the principal lens equation can be represented in linearized form as proposed by Kayser, Refsdal & Stabell (1986) and Paczyński (1986):

$$\vec{y}(\vec{x}) = \vec{x} - \begin{pmatrix} \sigma_* + \sigma_c + \gamma & 0 \\ 0 & \sigma_* + \sigma_c - \gamma \end{pmatrix} \vec{x} \quad (1)$$

where  $\vec{x}$  is a dimensionless coordinate in the lens plane, and  $\vec{y}$  is a corresponding coordinate in the source plane,  $\sigma_*$  is the normalized surface density of microlenses (stars), and  $\sigma_c$  is a surface density of any diffusely distributed matter. Parameter  $\gamma$  (shear) characterizes asymmetry of the gravitational field distribution in the region under consideration. In numerical simulation, the stellar constituent  $\sigma_*$  of the normalized surface density  $\sigma$  can be represented in an explicit form by an ensemble of microlenses randomly distributed in the macrolens plane, and then the previous formula can be written in the form:

$$\vec{y}(\vec{x}) = \vec{x} - \sum_i m_i \frac{\vec{x} - \vec{x}_i}{|\vec{x} - \vec{x}_i|^2} - \begin{pmatrix} \sigma_c + \gamma & 0 \\ 0 & \sigma_c - \gamma \end{pmatrix} \vec{x} \quad (2)$$

Here,  $\vec{x}(x_1, x_2)$  and  $\vec{y}(y_1, y_2)$  are the beam coordinates in the lens plane and in the source plane, respectively,  $\vec{x}_i$  is the coordinate of the  $i$ -th microlens (a star), and  $m_i$  is the microlens mass expressed in the units of the solar mass. All coordinates are dimensionless in this equation and are given in units of the Einstein radius of a single star, in the source plane and lens plane, respectively:

$$r_E^2 = \frac{4Gm D_S D_{LS}}{c^2 D_L}, \quad R_E^2 = \frac{D_L^2}{D_S^2} r_E^2. \quad (3)$$

Here,  $G$  is the gravitational constant,  $c$  is the velocity of light in the vacuum,  $m$  is a microlens mass, and  $D_{LS}$ ,  $D_L$ ,  $D_S$  are cosmological distances between the lens, the source, and the observer, (Schneider et al. 1992, Witt & Mao 1994).

Using equation (2), with the ray tracing method, (Schneider et al. 1992), it is possible to calculate the distribution of magnification rate  $M(y_1, y_2)$  for a small (quasi-point) source for all locations  $(y_1, y_2)$  – the so-called magnification map. In microlensing of a finite-size source, which is situated at the  $(y'_1, y'_2)$  point in the magnification map and is characterized by a surface brightness distribution  $B(y_1, y_2)$ , the magnification rate can be calculated from the formula:

$$\mu(y'_1, y'_2) = \frac{\int \int B(y_1, y_2) M(y_1 - y'_1, y_2 - y'_2) dy_1 dy_2}{\int \int B(y_1, y_2) dy_1 dy_2}, \quad (4)$$

where the integrals are calculated within a region where the surface brightness  $B(y_1, y_2)$  is non-zero. In this expression, we use the values of  $M(y_1, y_2)$  from the magnification map calculated for a quasi-point source. Specifying the source trajectory at the magnification map by the projections of its velocity  $V_1, V_2$  at the coordinate axis, one can calculate the corresponding simulated light curve:

$$m(t) = -2.5 \lg[\mu(y_{01} + V_1 t, y_{02} + V_2 t)] + C \quad (5)$$

where  $y_{01}, y_{02}$  are selected starting points of the trajectory.

One of the principal advantages of the ray tracing method is that, once calculated, the magnification map can be used to produce a large set of simulated light curves for various models of surface light distribution  $B(y_1, y_2)$  of a lensed source.

We simulated microlensing of a two-structure source, with one of them the compact, central luminous source having a surface brightness distribution  $B_1(y_1, y_2)$ . The other, outer, structure, is associated with the larger structural elements – a shell, a torus, Elvis's

biconics (Elvis 2000) – and is characterized by substantially lower surface brightness  $B_2(y_1, y_2)$ . For such a source, situated at point  $(y'_1, y'_2)$ , the values of the magnification rate  $\mu_{12}$  can be calculated from:

$$\mu_{12}(y'_1, y'_2) = \frac{\mu_1(y'_1, y'_2) + \varepsilon \mu_2(y'_1, y'_2)}{1 + \varepsilon}. \quad (6)$$

The magnification rates  $\mu_1$  and  $\mu_2$  are calculated according to (4) for the surface brightness distributions  $B_1$  and  $B_2$ , while  $\varepsilon$  is determined as a ratio of the integral luminosities of these structures:

$$\varepsilon = \frac{\int \int B_2(y_1, y_2) dy_1 dy_2}{\int \int B_1(y_1, y_2) dy_1 dy_2}. \quad (7)$$

The characteristic time-scale of observed Q2237 microlensing brightness fluctuations is known to be almost a year. We infer from known cosmological transverse velocities that such a scale is due to microlensing of the compact inner quasar structure. Since the predicted spatial scale of the outer structure is more than an order of magnitude larger as compared to the inner part, (Elvis 2000, Schild & Vakulik 2003), the expected time scale of its microlensing brightness variations should exceed ten years. So, because of the large dimension, the amplitudes of microlensing magnification should be noticeably less, as compared to microlensing of the compact structure. Thus we conclude, that on time-scales near 4 years, the magnification rate  $\mu_2(y_1, y_2)$  is almost unchanging and does not differ noticeably from the average magnification rate of the  $j$ -th component  $\mu_j$ , resulting from microlensing:  $\mu_2(y_1, y_2) \approx \langle \mu_2(y_1, y_2) \rangle \approx \mu_j$ . Under these assumptions, equation (6) can be rewritten:

$$\mu_{12}(y'_1, y'_2) = \frac{\mu_1(y'_1, y'_2) + \varepsilon \mu_j}{1 + \varepsilon}. \quad (8)$$

It is clear that, under such assumptions, microlensing of the extended (outer) structure does not produce noticeable variations of magnification or brightness fluctuations on the observationally sampled time-scales, and therefore is effectively a brightness plateau above which the inner structure brightness fluctuations are seen. So the observed inner region brightness fluctuations are reduced by  $1/(1 + \varepsilon)$ .

Therefore, when analysing the light curves for 4 year time intervals, we did not attempt to estimate the size of the extended structure, and the accepted value of  $\varepsilon$  was the only parameter which characterized the outer structure. The inner compact structure of the source was simulated by a disc with a Gaussian surface brightness distribution, and with its characteristic size  $r/r_E$  at the one-sigma level as a fitted parameter. We used this simple central source model because it is more easy for computation. In doing so, we relied on the work by Mortonson et al. (2005), who examined the effect of the source brightness profile on the observed magnitude fluctuations in microlensing. They used a variety of accretion disc models, including Gaussian disk, and concluded that the statistics of microlensing fluctuations is relatively insensitive to a particular light distribution over the source disk excepting the effective radius.

In producing magnification maps, microparameters  $\sigma_*$  and  $\gamma$  (shear) were taken from Kochanek (2004): 0.392, 0.375, 0.743, and 0.635 for  $\sigma_*$ , and 0.395, 0.390, 0.733, 0.623 for  $\gamma$ , for the A, B, C and D components, respectively. For each of the four Q2237+0305 components, we calculated five magnification maps with dimensions of 30 x 30 microlens Einstein radii, (a pixel scale of 0.02  $r_E$ ). We assumed here that the entire mass is concentrated only in stars – that is,  $\sigma_c$  equals zero. To simplify computations, all the stars were modeled as having the same mass. We are well aware that this assumption is rather artificial, but in doing so, we refer to

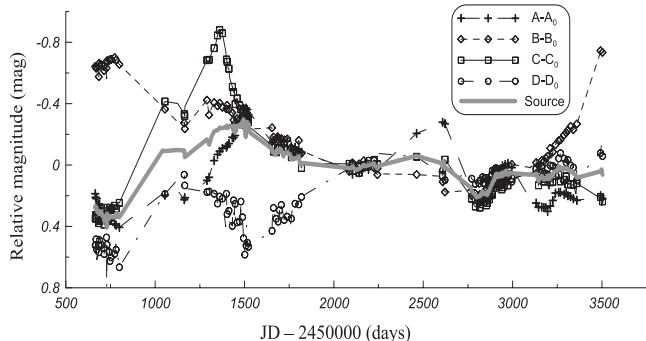


**Figure 1.** The OGLE light curves obtained in the V filter in 1997-2005. The light curves are reduced to the same (zero) level at the time interval JD 2090-2250. The solid grey line is our estimate of variations of the source brightness.

the works by Wambsgans (1992) and Lewis & Irwin (1995) who demonstrated, having used various mass functions, that the resulting magnification probability distributions are independent of the mass function of the compact lensing objects. For the sake of truth, the more recent works by Schechter, Wambsgans & Lewis (2004) and Lewis & Gil-Merino (2006) should be mentioned, where simulations with two populations of microlenses with noticeably differing masses were carried out to show that the magnification probability distributions can depend on the mass function. It is not surprising that such an exotic case has demonstrated the effect the authors wanted to demonstrate. But it is of little relevance for our work, since the more relevant calculation of Lewis & Irwin (1995) was made for more realistic mass functions – for microlenses in  $0.3M_{\odot}$ ,  $10.0M_{\odot}$  stars, and for the Salpeter mass function; these do not show appreciable dependence of the magnification probability distribution on the adopted mass function.

### 3 SIMULATION PROCEDURE AND RESULTS

For our analysis, we used the Q2237+0305 light curves obtained in the V filter by the OGLE group in 1997-2000. High sampling rate (2-3 datapoints weekly) and low random errors are inherent in the photometric data from this program. To compare with the simulated light curves, results of the OGLE photometry were averaged within a night, thus providing 108 data points in the light curve of each image component. For every set of the source model parameters, we estimated the probability to produce close approximations to the observed brightness curves. The values of the source model parameters providing the maximum probabilities, were accepted as the parameter estimates. To estimate consistency of the results, the analysis was carried out for each of the four image components separately.

Quasars are known to be variable objects, and their luminosity may change noticeably on time-scales of several years, months, and even days, (De Vries 2005, Gopal-Krishna et al. 2003, Rabbette et al. 1998). If a variable source is macrolensed, the intrinsic brightness variations will be observed in each lensed image with some time delays. This is just the fact that allows the Hubble constant to be determined from measurement of the time delays. In analysing microlensing, however, variability of the source is an interfering factor, which needs to be taken into account. In the Q2237+0305 system, because of an extreme proximity of the lensing galaxy, ( $z = 0.04$ ), and because of the almost symmetric lo-

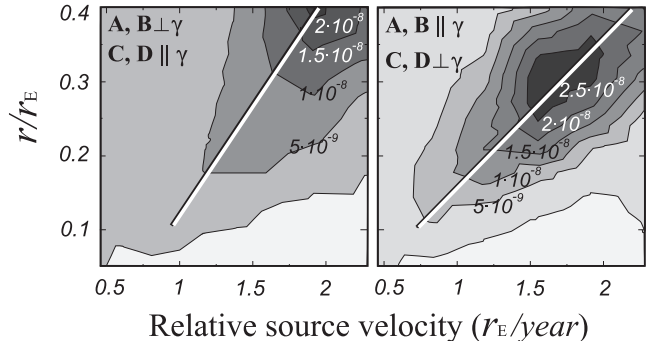


**Figure 2.** Probability distributions to find "good" simulated light curves as functions of the scaling factor and relative dimension of the compact feature. The diagrams are built for all the four components of Q2237+0305 for two directions of the source motion (as indicated on both panels in the left bottom corner). The probability scale is shown in levels of grey.

cations of the macroimages with respect to the lens galaxy center, the expected time delays do not exceed a day, (e.g. Wambsgans & Paczyński 1994, Schmidt et al. 1998). This is why the intrinsic brightness variations of the source would reveal themselves as almost synchronous variations of brightnesses of all the four lensed images. This was observed in 2003, (Vakulik et al. 2006), when the microlensing activity was substantially subdued for all four image components.

Generally, separation of the intrinsic brightness variations of the source from the light curves containing microlensing events is a poorly defined and intricate task. In our attempts to obtain the intrinsic source light curve for Q2237+0305, we introduced the following assumptions:

1. No effects of microlensing on the brightnesses of the components were observed during the time interval from January to June, 2002, (JD 2090-2250), when the magnitudes of all the components were almost unchanged. The magnitude of each component was accepted as a zero level, and its brightness variations were analysed relative to this level.

2. Relative to this zero level, we regarded that the closer these light curves were to each other, the higher the probability that the components are not microlensed within this time interval, while almost synchronous variations of their brightness are due to changes of the quasar brightness. And vice versa, the more the light curve of a component deviates from others, the larger the probability that the component is subjected to microlensing, which veils and distort the source variations.

Thus, the weighted average variations of the component brightnesses with respect to their zero levels were adopted as the estimate of the source brightness curve, with the statistical weight for variations of every component being selected depending on how close this brightness variation to variations of other components is. The quasar intrinsic brightness curve, obtained on the basis of these assumptions, as well as the OGLE light curves for the individual images, reduced to their zero levels, are shown in Fig. 1. We expect the largest source of error in this intrinsic source brightness history to be encountered during the time interval from August 1998 to December 1999, when, possibly, all the components underwent microlensing.

To characterize similarity of the simulated and observed light curves, a  $\chi^2$  statistics for each image component was chosen:

$$\chi_j^2 = \sum_j \frac{[m_j(t_i) - M_j(t_i, \vec{p})]^2}{\sigma_j^2}, \quad (9)$$

where  $m_j(t_i)$  is the observed light curve of the  $j$ -th component, and  $M_j(t_i, \vec{p})$  is one of the simulated light curves, produced from a source trajectory at the magnification map, and  $N_S$  is a number of points in the observed light curve. The magnification map was calculated for the source model described by a set of parameters  $\vec{p}$ , which could be varied. The quantity  $\sigma_j^2$  characterizes the errors of the observed light curve measurements, which are  $0.032^m$ ,  $0.039^m$ , and  $0.038^m$  for the A, B and C components, and  $0.057^m$  for the faintest D component.

The probability that, for a given set of parameters  $\vec{p}$ , a simulated light curve will be close enough to the observed light curve, – that is, the value of  $\chi^2$  will happen to be less than some boundary value  $\chi_0^2$ , – such a probability will be:

$$P(\chi^2 < \chi_0^2) = \frac{N_{\chi^2 < \chi_0^2}}{N_{tot}}, \quad (10)$$

where  $N_{\chi^2 < \chi_0^2}$  is a number of successful trials, and  $N_{tot}$  is a total number of trials. The boundary value  $\chi_0^2/N_S = 3$  was adopted for calculations.

The direction of an image motion with respect to the shear is an important parameter, which affects the probabilities noticeably. In (Kochanek 2004), directions of motion of each component were chosen randomly and independently of directions of other components. This is not quite correct, since the directions of motion of components are not independent, and are determined by the motion of the source. Therefore, specifying the motion of one of the components must automatically specify motions of other components, if the bulk velocities and velocity dispersion of microlenses can be neglected (Wambsganss & Kundić 1995, Wyithe et al. 2000). As a result of almost perfect symmetry of Q2237+0305, for any direction of the source motion, directions of the opposite components with respect to the shear direction must coincide, while motion for the two other images must be perpendicular to the shear direction. That's why, unlike the work by Kochanek (2004), we analysed trajectories for two selected directions at the magnification maps, – when the A and B components are moving along the shear, with the C and D moving transversely to it, and vice versa, when A and B are moving transversely to the shear. Also, we did not undertake the local optimization of trajectories, as in Kochanek (2004), since this may distort the estimates of probabilities.

Thus, for each magnification map, and for each of the two selected directions, a map of the distribution of the initial points of the trajectories can be calculated, for which  $\chi^2 < \chi_0^2$ . The probability (10) can then be calculated as the relative area of such regions on the map.

To reduce computing time, the map of  $\chi^2$  was calculated initially with a coarse mesh, ( $\sim 0.3 r/r_E$ ), to localize the regions with low values of  $\chi^2$ . Then, more detailed calculations with a finer mesh were carried out for only these regions.

In our simulation, the following parameters could be varied: the radius of the central compact feature  $r$ , expressed in units of a microlens Einstein radius  $r_E$ ; the brightness ratio,  $\varepsilon$ , expressing the ratio of the total outer structure (Elvis structure) brightness to the total inner structure brightness; and the relative transverse velocity of the source,  $V_t(r_E/\text{year})$ , expressed in the units of the Einstein radius of a microlens per year, which is also a scaling factor for simulated light curves.

The search of probabilities for our three fitting parameters,  $r/r_E$ ,  $\varepsilon$  and  $V_t$  is a rather complicated task, which needs much com-

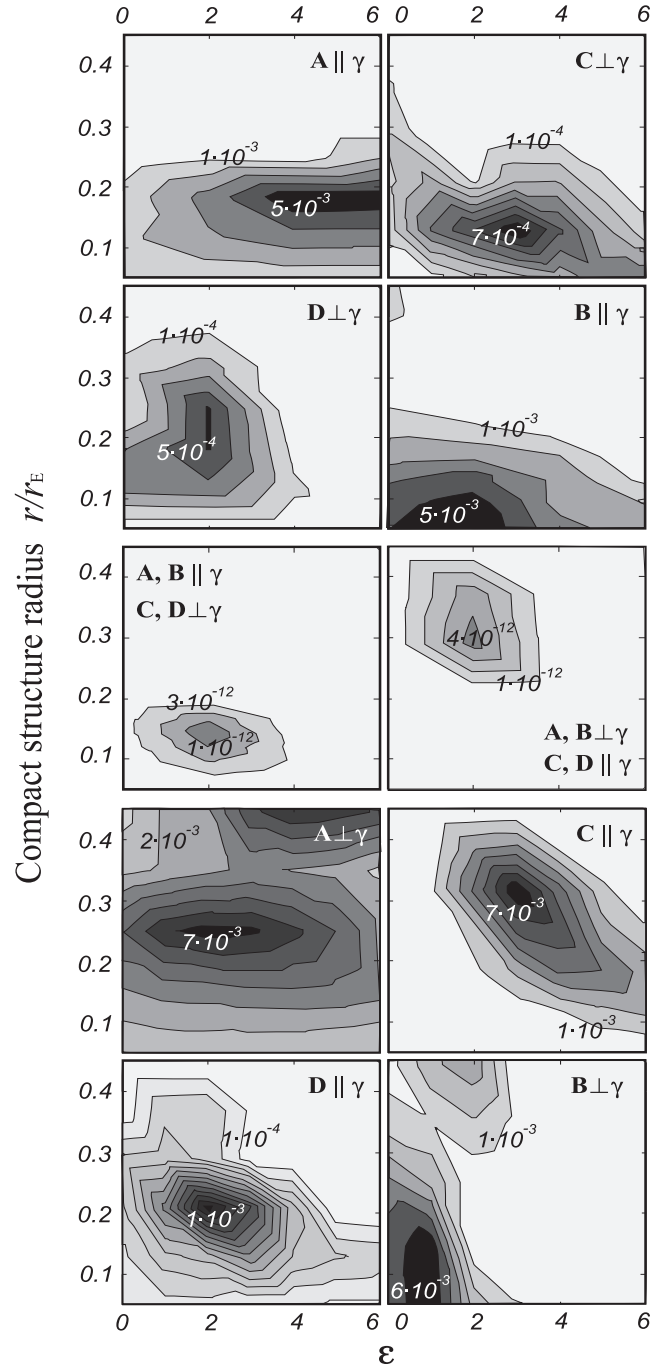


**Figure 3.** Probability distributions to find "good" simulated light curves as functions of the compact structure dimension,  $r/r_E$ , and of the ratio  $\varepsilon$  of the integral brightnesses of the outer and inner source structures. Rows 1 and 2: images C and D move along the shear, A and B transversely. Rows 4 and 5: A and B move parallel to the shear, C and D – transversely. The panels in the 3-d row show the joint probability distributions for the four components, for the two directions of the source motion.

puting time. We attempted to simplify it in the following way. Assuming that the effect of the outer structure on the characteristic time scales of microlensing brightness variations is insignificant, we put  $\varepsilon = 0$  at the first stage. Hence, a dependence of probabilities on two parameters, – the scaling factor and relative dimension of the compact feature, – was evaluated at the first stage. In Fig.2, the diagrams are presented, which demonstrate distributions of proba-

bilities to find simulated light curves, which would be close to the observed ones, – depending on the scaling factor and the compact feature dimension. The diagrams are built for all the four components for two directions of the source motion: A and B along the shear, C and D transversely – at the left, and C and D along the shear, A and B transversely – at the right. Overall, a nearly linear dependence of the scaling factor from the source dimension is seen. The largest values of probability occur for  $r/r_E \approx 0.4$  in the first case, and for  $r/r_E \approx 0.3$  in the second case. Since the maximum of probability distribution is, on average, at the source radius of  $0.35 r_E$  and the velocity of  $1.82 r_E$  per year (see Fig. 2), and taking into account a nearly linear dependence between these values, we adopted the following expression for the further calculations:

$$V_i = 1.82^{+1.18}_{-0.52} \frac{r/r_E}{0.35}. \quad (11)$$

Here, the source velocity  $V_i$  is expressed in the units of the microlens Einstein radius per year.

At the second stage of our simulation, the distribution of the probabilities to find simulated light curves similar to the observed ones was estimated, depending on the source’s compact feature dimension  $r/r_E$ , and on the relative integral brightness of the outer feature  $\varepsilon$ . The scaling factor  $V_i$  was determined according to (11) for each determination of the source dimension. The diagrams constructed for two different directions of the source motion, – along the shear  $\gamma$  and transversely to it for each component, – are shown in Fig. 3. Joint probability distributions for all the four components, calculated as  $P_{all} = P(A)P(B)P(C)P(D)$ , are also shown in the third row in this figure.

It is very significant that the probability maxima for all the components are found for values of  $\varepsilon$  larger than zero. This means that the outer quasar structures must noticeably contribute to the total quasar brightness in the optical wavelengths. The contribution decreases the amplitudes of microlensing brightness fluctuations and is at the core of the conundrum that in Q2237, observed microlensing events are lower in amplitude than inferred for simple luminous accretion disc models.

Interestingly, we also see from Fig. 3 that the statistics and locations of probability maxima in the domain of parameters  $\varepsilon$  and  $r/r_E$  found for each of the components separately, differ for different directions of motion of the image components with respect to the lens shear,  $\gamma$ . Examining four upper and four bottom panels of our Fig. 3, we see that the values of probabilities for the A and B components at their maxima are almost the same for the two selected directions of the source motion, while the C and D components both exhibit higher probabilities for the source to move parallel to the line connecting C and D rather than A and B. However, the joint probabilities calculated for all the four components, (the third row panels of Fig. 3), though giving slightly differing values of  $\varepsilon$  and  $r/r_E$ , favor neither of these two cases in terms of the maximal values of probabilities. Much larger statistics is needed to solve this important problem, which is beyond our current computational resources.

In Fig. 4, some of the most successful simulated light curves are shown together with the corresponding observed light curves reduced to their zero level. (The quasar light variations have been subtracted as described previously). It should be noted that the simulated light curves reproduce the observed ones well enough within the time interval of the fitting, and no unacceptably large brightness fluctuations are observed outside this interval, unlike the results in Fig. 10 of Kochanek (2004).

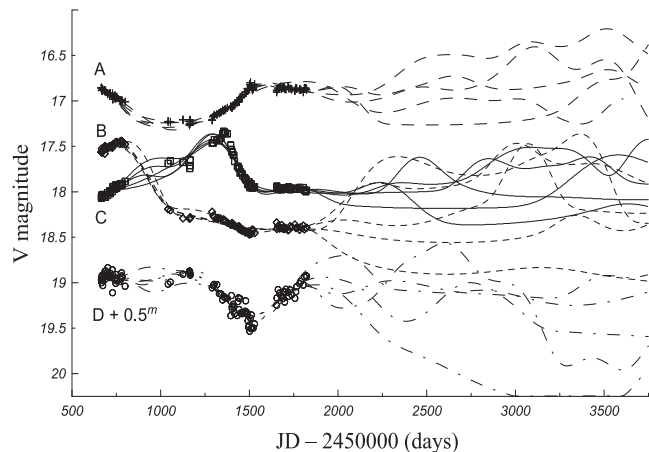


**Figure 4.** Some of the most successful simulated light curves plotted against the observed light curves. Microlensing brightness fluctuations beyond the time interval of fitting are approximately of the amplitude and duration observed.

## 4 CONCLUSIONS

In our Q2237 simulations, we have adopted a somewhat simplified version of the empirical quasar structure model successfully applied to Q0957 data by Schild & Vakulik (2003). We find that our source model consisting of a compact inner structure and much larger outer structure with lower surface brightness, allows us to avoid the effect from the standard accretion disc model that large amplitude microlensing brightness fluctuations are predicted but not observed, (Jaroszyński et al. 1992, Kochanek 2004). We used the method of statistical trials to determine the inner source dimensions and the contribution of the outer extended structure to the total quasar UV-optical luminosity.

Summarizing, we conclude:

- The proposed source model consisting of two structures, – an inner compact structure and an extended outer region, – provides higher values of probability to find “good” simulated light curves as compared to the central compact source alone, and produces better fits to long-term light curves.

- We found out that the probability distributions calculated for separate image components with two different directions of macroimage motion with respect to the shear  $\gamma$  are somewhat different. In principle, this fact might be a clue to determination of the direction of the source transverse motion relative to the shear in Q2237+0305. Further progress in this important area will require observation of many more microlensing events, and many more simulations over longer time intervals; this will require greater computational power. We find that, at the current stage of the investigation, there is no possibility to solve the problem, since the maxima of the joint (over all components) probability distributions differ insignificantly for the two selected directions of the source motion, (see Fig. 3).

- The calculated distributions of the joint probabilities has well-marked maxima, and their locations in the domain of parameters  $\varepsilon$  and  $r/r_E$  allow reasonable confidence in their determined values which provide the best fit of the simulated light curves to the observed ones. The range for the most probable values of the relative luminosity  $\varepsilon$  of the extended feature, determined from probability distributions of the individual macroimages, is between 1 and 3, while the estimate of the relative size of the compact central fea-

ture of the quasar varies within a range of  $0.1 < r/r_E < 0.45$ . When determined from distributions of the joint probabilities, the values of  $\varepsilon$  equal 2 in both cases, while  $r/r_E$  is about 0.4 for A and B motion perpendicular to  $\gamma$ , and 0.15 for A and B moving parallel to the shear  $\gamma$ .

- Very significantly, the simulated light curves calculated for the proposed two-component source model with the parameters indicated above, do not tend to unacceptably increase their amplitudes outside the time interval where they were objectively selected according to the  $\chi^2 < \chi_0^2$  criterion, as is seen in Fig. 10 from the work by Kochanek (2004).

- For better comparison, we adopted, following Kochanek (2004), a probable projected cosmological transverse source velocity of  $V_t = 3300$  km/s to determine a linear size of the compact central source of  $r \approx 2 \cdot 10^{15}$  cm, ( $1.2 \cdot 10^{15}$  cm  $< r < 2.8 \cdot 10^{15}$  cm). This size was estimated by Kochanek (2004) to be between  $r \approx 1.4 \cdot 10^{15} h^{-1}$  cm and  $4.5 \cdot 10^{15} h^{-1}$  cm for the accretion disc model and for the same transverse velocity, ( $h = 100/H_0$ , where  $H_0$  is the expected value of the Hubble constant). For the relative size of the source of  $0.3r_E$ , ( $0.1r_E < r < 0.45r_E$ ), the estimate for the average microlens mass is  $\langle m \rangle = 1.88 \cdot 10^{-3} h^2 M_\odot$ , ( $3.08 \cdot 10^{-4} h^2 M_\odot < \langle m \rangle < 3.3 \cdot 10^{-2} h^2 M_\odot$ ).

Thus we conclude that the proposed two-component model of the Q2237+0305 quasar structure provides better fit to the actual light curves of the four lensed quasar images as compared to the case of a compact central source alone. The importance of the extended structure for microlensing simulations was suspected for the first time more than ten years ago, (Jaroszyński et al. 1992, Witt & Mao 1994), and was successfully demonstrated for Q0957+561 by Schild & Vakulik (2003). Recently, the analysis of the X-ray and optical flux ratio anomalies in ten quadruply lensed quasars has made Pooley et al. (2007) deduce, that the optical radiation comes from a region much larger than that expected from the thin disk model by a factor of up to 30. Thus quasar microlensing studies at X-ray and optical wavelengths are converging to show that standard accretion disc models must be supplemented with an extended outer structure, contributing a noticeable fraction of the UV-optical continuum, and the present report shows how the comparison of simulations to microlensing observations demonstrates good fit and produces a determination of the size of the luminous inner quasar structure and its contribution to the total emission.

## ACKNOWLEDGMENTS

This work has been supported by the STCU grant U127. The authors are grateful to the unknown referee for very useful critical remarks and suggestions.

## REFERENCES

Abajas C., Mediavilla E., Munoz J.A., Gómez-Álvarez P., Gil-Merino R., 2007, ApJ, 658, 748  
 Agol E., Jones, B., Blaes O., 2000, ApJ, 545, 657  
 Antonucci R., 1993, Ann. Rev. Astron. Astrophys, 31, 473  
 Chelouche D., 2005, ApJ, 629, 667  
 de Vries W.H., Becker R.H., White R.L., Loomis C., 2005, AJ, 129, Iss. 2, 615  
 Elvis M., 2000, ApJ, 545, 63  
 Falco E.E., Lehár J., Perley R.A., Wambsganss J., Gorenstein M.V., 1996, AJ, 112, 897

Ferland G.J., Rees M. 1988, ApJ, 332, 141  
 Gil-Merino R., González-Cadelo J., Goicoechea L.J., Shalyapin V.N., Lewis G.F. 2006, MNRAS, 371, 1478  
 Gopal-Krishna, Stalin C.S., Sagar R., Wiita P.J., 2003, ApJ, 586, L25  
 Gould A., Miralda-Escudé J., 1997, ApJ, 483L, 13  
 Jaroszyński M., Wambsganss J., Paczyński B., 1992, ApJ, 396, L65.  
 Kaspi A., Smith P. S., Netzer, et al., 2000, ApJ, 533, 631  
 Kayser R., Refsdal S., Stabell R., 1986, A&A, 166, 36  
 Kochanek C.S., 2004, ApJ, 605, 58  
 Laor A., Netzer H. 1989, MNRAS, 238, 897  
 Lewis G.F., 2004, MNRAS, 355, 106  
 Lewis G.F., Ibata R.A., 2004, MNRAS, 348, 24  
 Lewis G., Ibata R.A., 2006, MNRAS, 367, 1217  
 Lewis G.F., Irwin M.J., 1995, MNRAS, 276, 103  
 Lewis G.F., Irwin M.J., 1996, MNRAS, 283, 225  
 Lewis G.F., Gil-Merino R. 2006, ApJ, 645, 835  
 Lewis G.F., Irwin M. J., Hewett P. C., Foltz C. B., 1998, MNRAS, 295, 573  
 Mediavilla E., Arribas S., del Burgo C., et al., 1998, ApJ, 503, L27  
 Mortonson M.J., Schechter P.L., Wambsganss J., 2005, ApJ, 628, 594  
 Paczyński B., 1986, ApJ, 301, 503  
 Pooley, D. et al, 2007, ApJ, 661, 19  
 Rabbette M., McBreen, B., Smith N., Steel S., 1998, A&AS, 129, 445  
 Racine R., 1992, ApJ, 395, L65  
 Rauch K., Blandford R., 1991, ApJ, 381, L39  
 Richards G.T., Keeton C. R., Pindor B. et al., 2004, ApJ, 610, 679  
 Saust A.B., 1994, A&ASS, 103, 33  
 Schechter P.L., Udalski A., Szymański M., et al., 2003, ApJ, 584, 657  
 Schechter P.L., Wambsganss J., Lewis G.F. 2004, ApJ, 613, 77  
 Schild R. E., 2005, AJ, 129, 1225  
 Schild R., Leiter D., Robertson S., 2006, AJ, 132, 420  
 Schild R., Vakulik V., 2003, AJ, 126, 689  
 Schmidt R., Webster R.L., Lewis G.F., 1998, MNRAS, 295, 488  
 Schneider P., Ehlers J., Falco E.E. Gravitational Lenses. Berlin - Heidelberg - New York, Springer-Verlag, 1992.  
 Shalyapin V.N., Goicoechea L.J., Alcalde D, et al. 2002, ApJ, 579, 127  
 Vakulik V.G., Schild R.E, Dudinov V.N., et al., 2004, A&A, 420, 447  
 Vakulik V.G., Schild R.E., Dudinov V.N., et al., 2006, A&A, 447, 905  
 Wambsganss J., Paczynski B., Schneider P., 1990, ApJ, 358, L33  
 Wambsganss J., Paczyński B., 1991, AJ, 102, 864  
 Wambsganss J., 1992, ApJ, 386, No.19, 19  
 Wambsganss J., Paczynski B., 1994, AJ, 108, 1156  
 Wambsganss J., Kundić T., 1995, ApJ, 450, 19  
 Wayth R.B., O'Dowd M., Webster R.L., 2005, MNRAS, 359, 561  
 Webster R.L., Ferguson A. M. N., Corrigan R. T., Irwin M. J., 1991, AJ, 102, 1939  
 Witt J.H., Mao S., 1994, ApJ, 429, 66  
 Wyithe J.S.B., Webster R.L., Turner E.L., 1999, MNRAS, 309, 261  
 Wyithe J.S.B., Webster R.L., Turner E.L., 2000, MNRAS, 312, 843  
 Yonehara A., 2001, ApJ, 548, L127